JOURNAL OF PHYSICAL ORGANIC CHEMISTRY
J. Phys. Org. Chem. 2005; **18:** 1099–1106
Published online 3 August 2005 in Wiley InterScience (www.interscience.wiley.com). DOI: 10.1002/poc.972

The electronic spectra of 2-(2′-hydroxybenzoyl)pyrrole and 2-(2′-methoxybenzoyl)pyrrole: a theoretical study

Giovanni Ghigo,[1]* Maurizio Ciofalo,[2] Laura Gagliardi,[3] Gianfranco La Manna[3] and Christopher J. Cramer[4]

[1]Dipartimento di Chimica Generale ed Organica Applicata, Università di Torino, C.so M. d'Azeglio 48, I-10125 Torino, Italy
[2]Dipartimento ITAF, Università di Palermo, Viale delle Scienze, Edificio 4, I-90128 Palermo, Italy
[3]Dipartimento di Chimica Fisica 'F. Accascina', Università di Palermo, Viale delle Scienze—Parco d'Orleans II, I-90128 Palermo, Italy
[4]Department of Chemistry and Supercomputer Institute, University of Minnesota, 207 Pleasant St. SE, Minneapolis, MN 55455-0431, USA

Received 1 April 2005; revised 24 May 2005; accepted 3 June 2005

ABSTRACT: The gas-phase electronic spectra of 2-(2′-hydroxybenzoyl)pyrrole and 2-(2′-methoxybenzoyl)pyrrole have been determined using multiconfigurational perturbation theory (CASPT2). Solvatochromic spectral shifts for these molecules have been measured in cyclohexane and methanol and the electrostatic components of these shifts have been estimated using the vertical electrostatic model (VEM 4.2) developed for the configuration interaction with single excitations model implemented with the intermediate neglect of differential overlap Hamiltonian (CIS/INDO/S2). Comparison between theory and experiment and an interpretation of the main spectral differences between the two substituted pyrroles and their solvation are presented. Copyright © 2005 John Wiley & Sons, Ltd.
Supplementary electronic material for this paper is available in Wiley Interscience at http://www.interscience.wiley.com/jpages/0894-3230/suppmat/

KEYWORDS: electronic spectra; solvatochromic shift; benzoylpyrrole; CASPT2; VEM; CIS/INDO/S2

INTRODUCTION

2-(2′-Hydroxybenzoyl)pyrrole (HBP, Fig. 1), a conformationally flexible aromatic system, is present as a substructure in a series of halogenated, naturally occurring[1] and synthetic[2,3] pyrroles with remarkable bactericidal activity, and in some recently synthesized cytotoxic 2-aroylindoles with promising antitumour activities.[4,5] The O-methylation of the hydroxyl group, giving rise in HBP to 2-(2′-methoxybenzoyl)pyrrole (MBP, Fig. 2), and the N-substitution of the pyrrole moiety in bioactive compounds structurally similar to HBP and MBP were shown to reduce the antibiotic activity while their cytotoxic action still operates.[6] On the other hand, the presence of a free OH group has some noticeable effects on the physical behaviour of these benzoylpyrroles. In fact, although chemically pure HBP is a yellow crystalline substance, its *O*-methyl derivative MBP is white; the same contrast is observed for their solutions in both polar and non-polar solvents. In a previous paper[7] we investigated the tautomeric and conformational equilibria of HBP and MBP using quantum chemical methods. We also determined their infrared spectra both experimentally and theoretically. In this work, we focus on the electronic spectra of HBP and MBP to evaluate the extent to which chemical substitution and solvation effects influence the positions of various absorption maxima (the latter phenomenon typically is referred to as solvatochromism). The prediction of electronic excitation spectra can be a challenging task from a methodological standpoint and we assess the degree to which particular computational models are effective in the HBP and MBP systems. From a drug design standpoint, accurate prediction of UV–Vis spectra could prove useful for the engineering of improved photostability into effective pharmacophores, which is an economically important goal.

COMPUTATIONAL METHODS

The complete active space (CAS) SCF method[8] was used to generate molecular orbitals and reference wave functions for subsequent multiconfigurational second-order perturbation calculations of the dynamic correlation energy (CASPT2).[9–11] The active space was composed of 12 active electrons in 12 active orbitals. These orbitals include the five highest π and the five lowest π^* orbitals that are delocalized on the pyrrole (π_{Py}) and phenyl (π_{Bz})

**Correspondence to:* G. Ghigo, Dipartimento di Chimica Generale ed Organica Applicata, Università di Torino, C.so M. d'Azeglio 48, I-10125 Torino, Italy.
E-mail: giovanni.ghigo@unito.it
Contract/grant sponsor: Italian Ministero dell'Istruzione dell'Università e della Ricerca (MIUR).
Contract/grant sponsor: US National Science Foundation; *Contract/grant number:* NSF CHE02-03346.

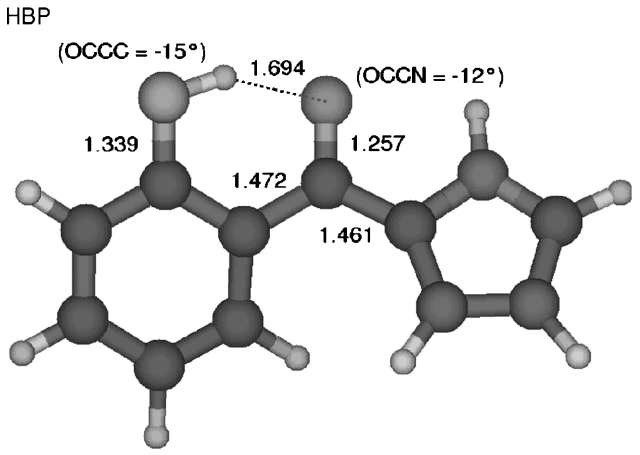

Figure 1. The calculated structure of 2-(2′-hydroxybenzoyl)pyrrole (HBP). Bond distances are in angstroms and angles are in degrees

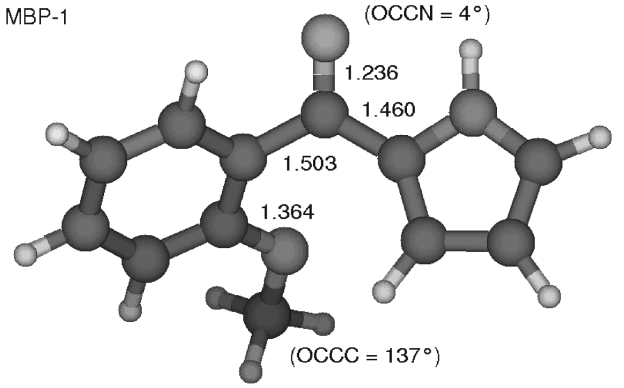

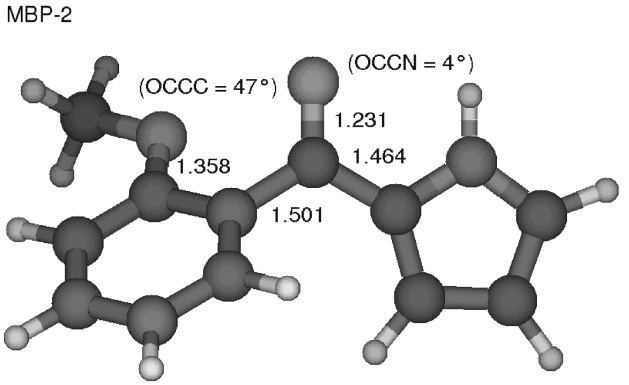

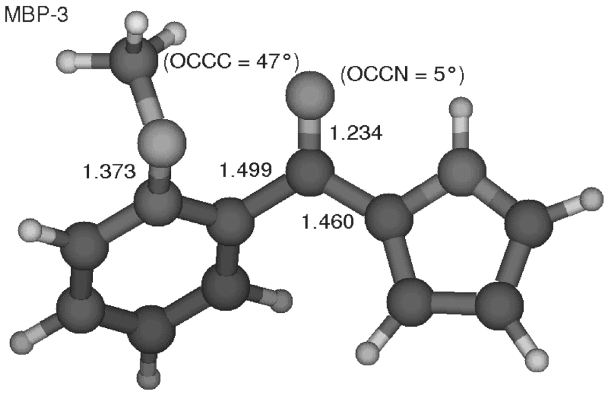

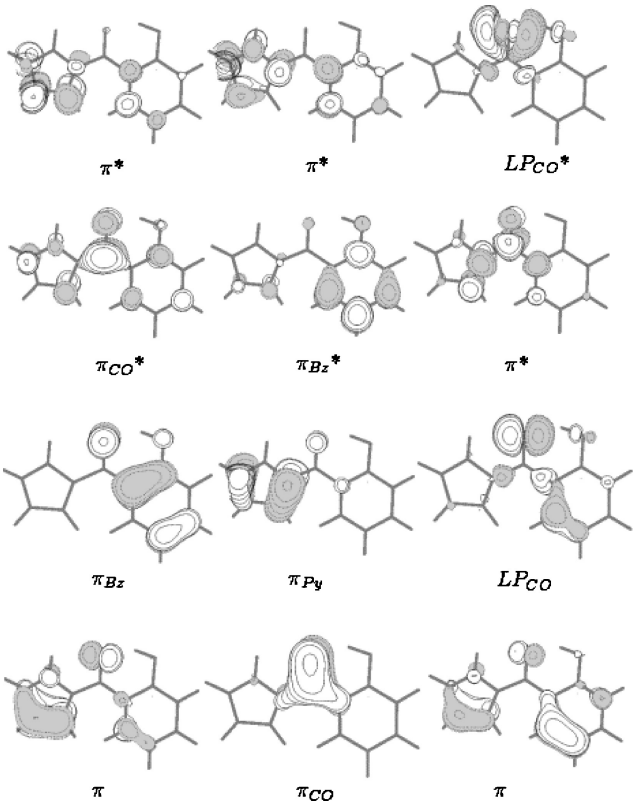

Figure 3. The active molecular orbitals of 2-(2′-hydroxybenzoyl)pyrrole (HBP)

moieties and on the carbonyl group (π_{CO}). The lone-pair orbital localized on the oxygen of the carbonyl group (LP_{CO}) and a second orbital (LP_{CO}*), which reduced a serious intruder state problem, were also considered. The active molecular orbitals for HBP are shown in Fig. 3. Some residual intruder states were still present but it was not possible to extend the active space further due to the size of the molecule and the absence of any symmetry that would reduce the computational effort. In any case, the agreement with experiment did not appear to be compromised by the remaining intruder states.

The molecular orbitals were optimized for the first six singlet states in a State-Average CASSCF calculation. The excitation energies then were computed at the CASPT2 level of theory. The CASSCF wavefunctions, combined with the CASPT2 excitation energies, were used to estimate the oscillator strengths of the excitations. Generally contracted basis sets of atomic natural orbital (ANO) type were used with the contraction scheme 3s2p1d on C, N and O and 2s1p on H.[12] The CASSCF/CASPT2 calculations were performed using the software MOLCAS-6.0.[13]

Electrostatic components of solvation free energies were computed from generalized Born (GB) quantum

Figure 2. The calculated structure of the three conformers of 2-(2′-methoxybenzoyl)pyrrole (MBP-1, MBP-2 and MBP-3). Bond distances are in angstroms and angles are in degrees

mechanical self-consistent-reaction-field (SCRF) calculations[14] for both the ground and excited states. Ground-state wave functions were determined from Hartree–Fock calculations with the semi-empirical intermediate neglect of differential overlap[15] Hamiltonian INDO/S2.[16] Excited-state wave functions were computed with the same Hamiltonian from configuration interaction calculations including single excitations (CIS).[15] The ground- and excited-state charge distributions were expressed as a monopole expansion of partial atomic charges (Charge Model 2—CM 2[16,17]) that were then used in the GB calculations. For the ground states, SCRF calculations using Solvation model 5.42 (SM 5.42[18]) were fully equilibrated to the solute charge distribution, whereas for the excited states the vertical electrostatic model 4.2 (VEM 4.2[19]) was used. The two-response-time VEM 4.2 model separates the slow and fast components of the solvent dielectric response to reflect properly the vertical nature of the electronic excitation. The INDO/S2 calculations were performed using the software ZINDO-MN.[20]

All geometries were optimized at the hybrid Hartree–Fock density functional level of theory[21] with the exchange functional of Becke[22] and the gradient-corrected correlation functional of Lee, Yang and Parr[23] (B3LYP). The polarized 6–31G(d,p) basis set[24] was used. The optimizations were performed using Gaussian 98 software.[25]

Figures 1–3 and 5 were obtained with the MOLDEN program.[26]

RESULTS AND DISCUSSION

In our previous study[7] three isomers of HBP were investigated but a single structure was found to dominate at equilibrium (Fig. 1) because the other two structures were $>80\,\mathrm{kJ\,mol^{-1}}$ higher in energy. We decided to consider only this structure in the present study. Five conformers of MBP were investigated but two were too high in energy ($>8\,\mathrm{kJ\,mol^{-1}}$) to be present in significant concentration at 298 K. We thus considered only three conformers of the *O*-methyl derivative in this study (MBP-1, MBP-2 and MBP-3 in Fig. 2). At the CASPT2 level, MBP-2 and MBP-3 lie 4.1 and $5.2\,\mathrm{kJ\,mol^{-1}}$ above MBP-1, respectively. From these relative energies, the following relative concentrations at 298 K can be estimated: 76% for MBP-1, 15% for MBP-2 and 9% for MBP-3.

The most important geometrical parameters for the various structures are reported in Figs 1 and 2. Two main differences between HBP and MBP appear: the presence of an intramolecular hydrogen bond in HBP, which is absent in the MBP isomers, and reduced coplanarity between the carbonyl group and the phenyl group in the MBP isomers (the CCCO dihedral angle is 43–47°) compared with HBP (the CCCO dihedral angle is 15°), presumably due to the presence of the methyl group.

The experimental spectra (Fig. 4) of HBP and MBP recorded in cyclohexane (C_6H_{12}) and methanol (CH_3OH) were reported in our previous work.[7] The experimental spectrum of HBP in C_6H_{12} presents a broad band with two maxima at ca. 3.58 eV (346 nm) and 3.99 eV (311 nm) and a narrow band with a maximum at ca. 4.79 eV (259 nm). The spectrum of MBP in C_6H_{12} presents a band with a maximum at ca. 4.27 eV (290 nm) and a shoulder at ca. 5.00 eV (248 nm). Although the spectrum of HBP in CH_3OH is similar to that in C_6H_{12}, the spectrum of MBP shows a clear red shift in going from C_6H_{12} to CH_3OH: the band with the maximum at 4.27 eV (290 nm) occurs instead at 4.13 eV (300 nm) and the shoulder at 5.00 eV (248 nm) is shifted by 6 nm (254 nm).

Results from CASPT2

In Tables 1–4 the vertical excitation energies and oscillator strengths for the first five singlet excited states are reported. The nature of the transitions was established from analysis of the electron charge transfer from the pyrrole and the hydroxybenzoyl (methoxybenzoyl) moieties towards the carbonyl group and the changes of the molecular orbital occupations in the excited states compared with the ground state. For all species, vertical CASPT2 excitation energies are in an energy range of 3.5–5 eV above their ground states.

Inspection of Tables 1–4 shows that the $LP_{CO} \rightarrow \pi_{CO}^*$ transition has a low intensity in every case. It occurs at 3.95 eV (314 nm) in HBP and at 3.82–3.87 eV (325–321 nm) in the MBP conformers, and corresponds to the typical $n \rightarrow \pi_{CO}^*$ dipole-forbidden transition of carbonyl systems, e.g. formaldehyde (3.91 eV at the CASPT2 level)[27] and acetone (4.18 eV).[28] The vertical transition in malonaldehyde, which is also an unsaturated carbonyl system and presents the same type of intramolecular hydrogen bond as HBP, is estimated at 3.89 eV at the same level of theory.[29] In the MBP conformers this transition is 0.1 eV lower than in benzaldehyde (3.71 eV at the CASPT2 level).[30]

The first intense transition ($f = 0.3$), of $\pi_{Bz} \rightarrow \pi_{CO}^*$ type has been calculated at 3.53 eV (351 nm) in HBP and corresponds to the maximum at 346 nm of the broad band of the experimental spectrum in C_6H_{12} (Fig. 4). The structurally similar *o*-hydroxybenzaldehyde species has an absorption band measured at 3.9 eV (330 nm) in 3-methylpentane,[31] which is the analogue of the band at 346 nm of HBP. The CASPT2 calculations on *o*-hydroxybenzaldehyde[32] predict this band to occur at 3.74 eV (332 nm). The presence of the pyrrole ring in HBP is thus responsible for the smaller transition energy than that found for *o*-hydroxybenzaldehyde.

In the three conformers of MBP, the $\pi_{Bz} \rightarrow \pi_{CO}^*$ transition has been computed ca. 1 eV higher than in HBP: 4.39 (282), 4.47 (277) and 4.55 eV (273 nm), respectively, with a lower intensity ($f < 0.04$). This

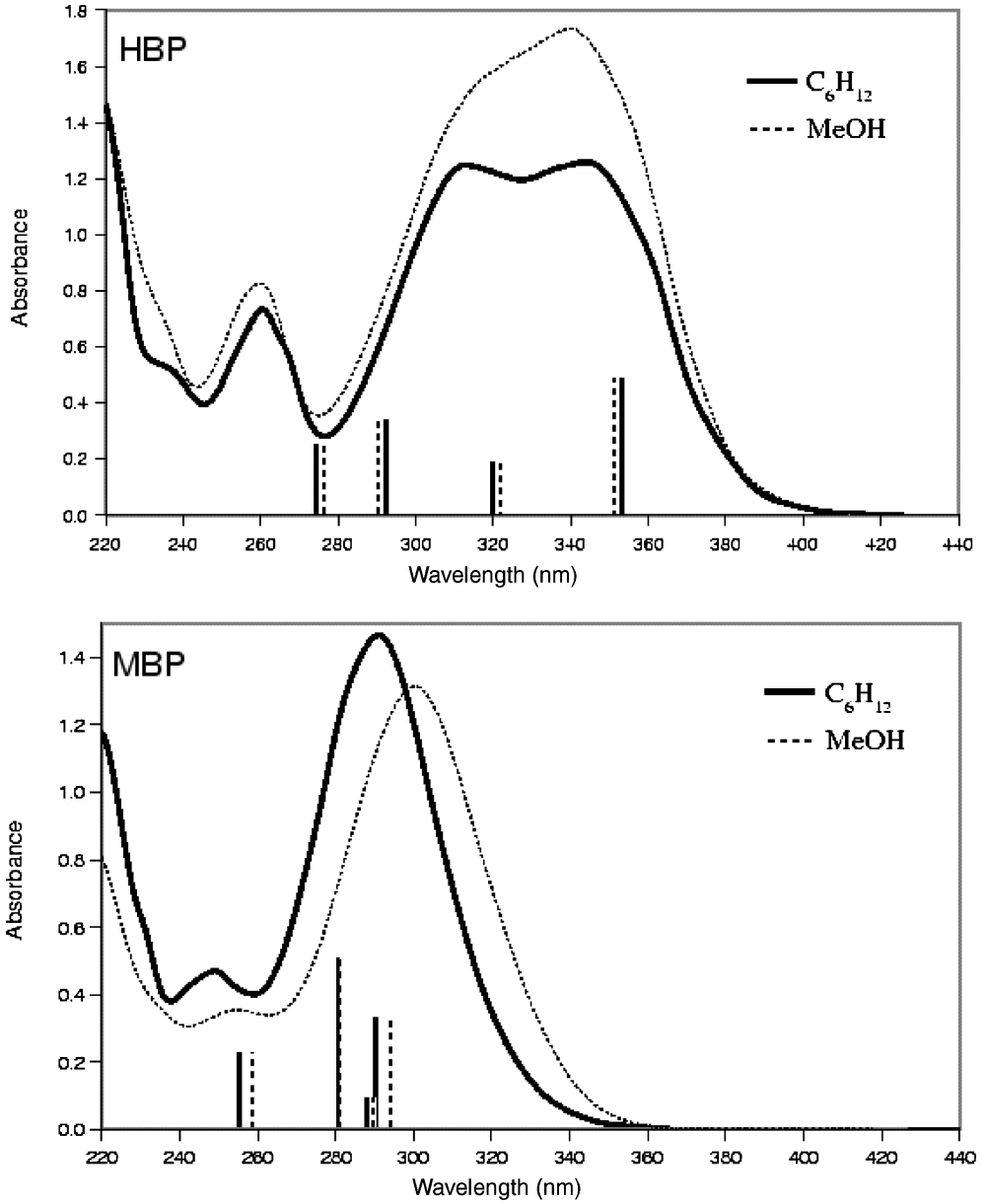

Figure 4. The measured spectra of HBP and MBP (absorbances are in arbitrary units) and the computed transitions (CASPT2 + VEM 4.2 solvatochromic shifts) for HBP and MBP-1 in C_6H_{12} and MeOH

difference between HBP and MBP is also present in the experimental spectra (Fig. 4): the band at 346 nm for HBP is absent in the MBP spectrum. This difference can be explained by looking at the changes in the molecular orbital (MO) occupations that occur upon transition in the two species. All transitions are single-electron excitations from some doubly occupied MOs mainly to the π_{CO}^* orbital. However, in the excited states of the MBP isomers there is considerable occupation of a π_{Bz}^* orbital (0.35–0.44) compared with the same excited state of HBP (<0.1), therefore the transition has some character of 'internal' benzene excitation, which is responsible for the

Table 1. Excitation energies, wavelengths and oscillator strengths (f) for HBP

Excitation	E (eV)	λ (nm)	f
$\pi_{Bz} \rightarrow \pi_{CO}^*$	3.53	351	0.271
$LP_{CO} \rightarrow \pi_{CO}^*$	3.95	314	0.007
$\pi_{Py} \rightarrow \pi_{CO}^*$	4.00	310	0.090
$\pi_{Py} \rightarrow \pi_{CO}^*$	4.45	278	0.165
$\pi_{Bz} \rightarrow \pi_{CO}^*$	4.75	261	0.124

Table 2. Excitation energies, wavelengths and oscillator strengths (f) for MBP-1

Excitation	E (eV)	λ (nm)	f
$LP_{CO} \rightarrow \pi_{CO}^*$	3.82	324	0.002
$\pi_{Py} \rightarrow \pi_{CO}^*$	4.31	287	0.163
$\pi_{Bz} \rightarrow \pi_{CO}^*$	4.39	282	0.038
$\pi_{Py} \rightarrow \pi_{CO}^*$	4.42	280	0.259
$\pi_{Bz} \rightarrow \pi_{CO}^*$	5.01	248	0.129

Table 3. Excitation energies, wavelengths and oscillator strengths (f) for MBP-2

Excitation	E (eV)	λ (nm)	f
$LP_{CO} \rightarrow \pi_{CO}^*$	3.82	324	0.001
$\pi_{Bz} \rightarrow \pi_{CO}^*$	4.47	277	0.038
$\pi_{Py} \rightarrow \pi_{CO}^*$	4.52	275	0.145
$\pi_{Py} \rightarrow \pi_{CO}^*$	4.58	271	0.309
$\pi_{Bz} \rightarrow \pi_{CO}^*$	4.90	253	0.103

Table 4. Excitation energies, wavelengths and oscillator strengths (f) for MBP-3

Excitation	E (eV)	λ (nm)	f
$LP_{CO} \rightarrow \pi_{CO}^*$	3.87	321	0.001
$\pi_{Py} \rightarrow \pi_{CO}^*$	4.46	278	0.144
$\pi_{Py} \rightarrow \pi_{CO}^*$	4.54	273	0.318
$\pi_{Bz} \rightarrow \pi_{CO}^*$	4.55	273	0.011
$\pi_{Bz} \rightarrow \pi_{CO}^*$	5.11	243	0.140

significant blue shift and the reduced intensity. The first singlet excited state of the benzene molecule occurs at 4.90 eV and its oscillator strength is very low (5×10^{-4}).[33] This behaviour could be due to the reduced coplanarity (and thus reduced conjugation) of the phenyl ring with the pyrrole and the carbonyl moieties, as noted above. A second $\pi_{Bz} \rightarrow \pi_{CO}^*$ transition has been found at higher energy: 4.75 eV (261 nm) for HBP, which corresponds to the low band observed in solution at 259 nm; and 4.9–5.1 eV (253–243 nm) for the MBP isomers with similar intensities, which corresponds to the 248 nm shoulder in solution. In the latter case the blue shift is only 0.25 eV and the populations of the π_{Bz}^* orbital in both the HBP and MBP isomers are similar.

In addition, two $\pi_{Py} \rightarrow \pi_{CO}^*$ transitions have been computed. In HBP, the first one occurs at 4.00 eV (310 nm) and corresponds to the maximum at 311 nm of the broad band in solution, whereas the second one is at 4.45 eV (278 nm). In the MBP conformers these two transition are computed at 4.31–4.52 eV, corresponding to a weighted average of 284 nm, and 4.42–4.58 eV (average = 278 nm) respectively, and their intensities are about twice the intensity in HBP. Together, they correspond to the intense band at 290 nm in solution, which is consistent with an observed absorption for 2-acetylpyrrole at 4.20 eV (287 nm).[34]

All transitions, with the exception of the first $\pi_{Bz} \rightarrow \pi_{CO}^*$, show a blue shift of ca. 0.1–0.4 eV in going from HBP to the MBP isomers. This is rationalized again in terms of the reduced coplanarity of the phenyl ring with the carbonyl group. The reduced coplanarity mitigates conjugation of the phenyl π orbitals with the π_{CO}^* orbital of the carbonyl group and thus the stabilization of the latter antibonding orbital. As a result, the energy of the π_{CO}^* orbital is 1.6 eV higher in the MBP isomers than in HBP. All transitions to this orbital thus occur at higher energy in the MBP isomers than in HBP.

Solvent effect

In order to estimate the solvent effects on the spectra, CIS/INDO/S2 calculations have been performed. At the DFT optimized geometries, the lowest six electronic states of HBP and the most stable conformer of MBP, MBP-1, have been calculated in the gas phase and in cyclohexane solution. Analogous calculations have been done for HBP and MBP-1, both with and without two explicitly coordinated methanol molecules in methanol solution. The structures of the supermolecular systems HBP + 2 MeOH and MBP-1 + 2MeOH (Fig. 5) were optimized previously at the DFT/B3LYP level of theory.

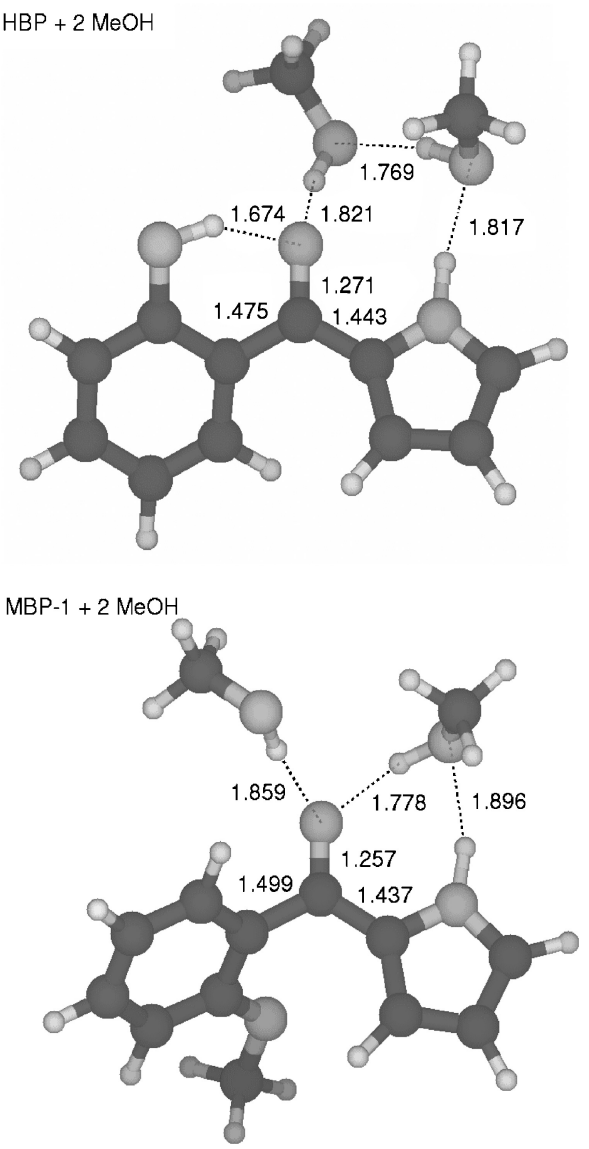

Figure 5. The calculated structure of 2-(2′-hydroxybenzoyl)pyrrole (HBP) plus two MeOH molecules and of 2-(2′-methoxybenzoyl)pyrrole (MBP-1) plus two MeOH molecules

Table 5. The ZINDO excitation wavelengths, oscillator strengths (f) and dipole moment (μ)[a] for HBP in the gas phase (gas), in cyclohexane (C_6H_{12}) and in methanol (MeOH), respectively

	Gas			C_6H_{12}		MeOH	
Excitation	λ(nm)	f	μ(D)	λ(nm)	μ(D)	λ(nm)	μ(D)
$LP_{CO} \rightarrow \pi_{CO}^*$	355	0.002	1.4	353	1.6	347	2.1
$\pi_{Bz} \rightarrow \pi_{CO}^*$	312	0.349	2.5	314	3.1	313	3.8
$\pi_{Py} \rightarrow \pi_{CO}^*$	278	0.244	8.7	288	9.0	289	9.0
$\pi_{Bz} \rightarrow \pi_{CO}^*$	236	0.031	4.7	249	5.0	248	5.5
$\pi_{Py} \rightarrow \pi_{CO}^*$	224	0.058	5.1	238	6.2	239	7.5

[a] The dipole moment for the ground state is 2.8, 3.1 and 3.9 D, respectively, in the gas phase, in cyclohexane and in methanol.

The results of these calculations have been summarized in Tables 5–10. The excitation wavelengths of HBP in the gas phase, cyclohexane and methanol are reported in Table 5 together with the dipole moments of each state. In going from gas to both solvents, the $LP_{CO} \rightarrow \pi_{CO}^*$ transition undergoes a blue shift whereas the intense $\pi_{Bz} \rightarrow \pi_{CO}^*$ and $\pi_{Py} \rightarrow \pi_{CO}^*$ transitions undergo a red shift. These changes are consistent with the nature of the polarities of the various excited states as measured by their dipole moments. In particular, the $LP_{CO} \rightarrow \pi_{CO}^*$ states have dipole moments smaller than the ground state, but all of the $\pi_{Bz} \rightarrow \pi_{CO}^*$ states have dipole moments larger than the ground state. For each set of states, the solvatochromic effect is larger for methanol than for cyclohexane because of the larger dielectric constant of the alcohol (32.6) compared with the alkane (2.0).

The excitation wavelengths for the HBP + 2MeOH system in gas and in methanol are reported in Table 6. In going from gas to methanol, the energy of the $LP_{CO} \rightarrow \pi_{CO}^*$ transition does not change whereas the $\pi_{Bz} \rightarrow \pi_{CO}^*$ and $\pi_{Py} \rightarrow \pi_{CO}^*$ transitions undergo a small red shift. Similar data for MBP-1 are reported in Tables 7 and 8.

The changes associated with computing solvatochromic effects in methanol using either isolated or microsolvated solutes are small, suggesting that it is reasonable to make a comparison between cyclohexane and methanol from purely continuum calculations. As a best estimate, then, to a prediction of the absorption maxima in solution, we have added the VEM 4.2 solvatochromic shifts to the CASPT2 gas-phase results; these data are provided in Tables 9 and 10 and are shown as bars in Fig. 4. The longest wavelength $\pi \rightarrow \pi_{CO}^*$ transition in HBP is predicted to occur 1 nm more to the blue in methanol compared with cyclohexane, which is consistent with the experimental spectrum that shows a very slight red shift for cyclohexane compared with methanol. The longest $\pi \rightarrow \pi_{CO}^*$ wavelength transition in MBP-1, on the other hand, is predicted to be shifted 3 nm more to the red in methanol compared with cyclohexane, and this again agrees with experiment, although the magnitude of the predicted shift is smaller than the 10 nm observed experimentally. The $LP_{CO} \rightarrow \pi_{CO}^*$ and $\pi_{Bz} \rightarrow \pi_{CO}^*$ transitions basically remain unchanged for HBP (Table 9) whereas the $\pi_{Py} \rightarrow \pi_{CO}^*$ transitions red-shift by ca. 10 nm from gas to cyclohexane and by 3 nm from gas to methanol. In going from cyclohexane to methanol a blue shift of 7 nm occurs. In the MBP-1 case (Table 10), in going from cyclohexane to methanol, a blue shift of 4 nm occurs for the lowest $\pi_{Bz} \rightarrow \pi_{CO}^*$ transition whereas all the other transition have small red shifts.

It is noteworthy that for certain excitations the solvatochromic shift for methanol is slightly more than twice what is predicted for cyclohexane, whereas in other cases the two solvents are predicted to have essentially equivalent solvatochromic shifts. This reflects the need to separate the solvent response into two components. The fast component, which involves the electronic response of the solvent, is essentially equivalent for cyclohexane and methanol and depends on the solvent index of refraction, which is 1.43 for cyclohexane and 1.33 for methanol, i.e. equivalent to within 7%. The slow component, on the other hand, which is frozen on the time scale of a vertical excitation, depends on the solvent dielectric constant. As noted above, the two solvents are substantially different with respect to this latter property. To a first approximation, then, if an excitation does not change the component of the solute dipole moment that is aligned with the slow component of the solvent reaction field, then one expects cyclohexane and methanol to exhibit a similar solvatochromic influence acting exclusively through their fast

Table 6. The ZINDO excitation wavelengths, oscillator strengths (f) and dipole moment (μ)[a] for HBP + 2 MeOH molecules in the gas phase (gas) and in methanol (MeOH), respectively

	Gas			MeOH	
Excitation	λ(nm)	f	μ(D)	λ(nm)	μ(D)
$LP_{CO} \rightarrow \pi_{CO}^*$	336	0.005	2.6	336	2.5
$\pi_{Bz} \rightarrow \pi_{CO}^*$	314	0.448	1.5	315	2.3
$\pi_{Py} \rightarrow \pi_{CO}^*$	288	0.152	4.7	291	4.8
$\pi_{Py} \rightarrow \pi_{CO}^*$	248	0.020	5.0	252	5.4
$\pi_{Bz} \rightarrow \pi_{CO}^*$	240	0.037	4.8	242	4.2

[a] The dipole moment for the ground state is 0.6 and 1.0 D, respectively, in the gas phase and in methanol.

Table 7. The ZINDO excitation wavelengths, oscillator strengths (f) and dipole moment (μ)[a] for MBP-1 in the gas phase (gas), in cyclohexane (C_6H_{12}) and in methanol (MeOH), respectively

	Gas			C_6H_{12}		MeOH	
Excitation	λ(nm)	f	μ(D)	λ(nm)	μ(D)	λ(nm)	μ(D)
$LP_{CO} \rightarrow \pi_{CO}^*$	336	0.004	1.8	333	2.1	326	2.8
$\pi_{Py} \rightarrow \pi_{CO}^*$	292	0.123	4.9	296	5.6	299	6.6
$\pi_{Bz} \rightarrow \pi_{CO}^*$	272	0.322	6.6	279	6.6	280	6.8
$\pi_{Bz} \rightarrow \pi_{CO}^*$	242	0.052	6.7	249	7.7	252	8.8
$\pi_{Py} \rightarrow \pi_{CO}^*$	231	0.198	4.7	232	5.4	232	5.9

[a] The dipole moment for the ground state is 3.2, 3.7 and 4.3 D, respectively, in the gas phase, in cyclohexane and in methanol.

Table 8. The ZINDO excitation wavelengths, oscillator strengths (f) and dipole moment (μ)[a] for MBP-1 + 2 MeOH molecules in the gas phase (gas) and in methanol (MeOH), respectively

	Gas			MeOH	
Excitation	λ(nm)	f	μ(D)	λ(nm)	μ(D)
$LP_{CO} \rightarrow \pi_{CO}^*$	327	0.015	4.4	326	4.8
$\pi_{Py} \rightarrow \pi_{CO}^*$	295	0.217	3.7	300	7.2
$\pi_{Bz} \rightarrow \pi_{CO}^*$	282	0.257	6.2	285	6.4
$\pi_{Bz} \rightarrow \pi_{CO}^*$	250	0.050	5.9	261	11.7
$\pi_{Py} \rightarrow \pi_{CO}^*$	233	0.124	10.7	235	7.0

[a] The dipole moment for the ground state is 4.4 and 5.3 D, respectively, in the gas phase and in methanol.

Table 9. The CASPT2 excitation wavelengths in the gas phase and the solvent effect shifts determined by ZINDO calculations for HBP (experimental values are in parentheses).

Excitation	Gas (nm)	C_6H_{12} (nm)	MeOH (nm)
$\pi_{Bz} \rightarrow \pi_{CO}^*$	351	353(346)	352(339)
$LP_{CO} \rightarrow \pi_{CO}^*$	314	312	306
$\pi_{Py} \rightarrow \pi_{CO}^*$	310	320(311)	321(312)
$\pi_{Py} \rightarrow \pi_{CO}^*$	278	292	291
$\pi_{Bz} \rightarrow \pi_{CO}^*$	261	274(259)	275(258)

Table 10. The CASPT2 excitation wavelengths in the gas phase and the solvent effect shifts determined by ZINDO calculations for MBP-1 (experimental values are in parentheses)

Excitation	Gas (nm)	C_6H_{12} (nm)	MeOH (nm)
$LP_{CO} \rightarrow \pi_{CO}^*$	324	321	314
$\pi_{Py} \rightarrow \pi_{CO}^*$	287	291(290)	294(300)
$\pi_{Bz} \rightarrow \pi_{CO}^*$	282	289	290
$\pi_{Py} \rightarrow \pi_{CO}^*$	280	281	281
$\pi_{Bz} \rightarrow \pi_{CO}^*$	248	255(248)	258(254)

response. Conversely, when a significant change in the solute charge distribution relative to the frozen component of the solvent reaction field occurs, one expects the two solvatochromic effects to differ by approximately $(\varepsilon - 1)/\varepsilon$ (the Born prefactor for the polarization free energy), and this is roughly a factor of 2 for cyclohexane versus methanol.[19]

CONCLUSIONS

The electronic spectra of HBP and three isomers of MBP have been computed using multiconfigurational perturbation theory and they are in good agreement with the experimental spectra.

The differences in the spectra of HBP and MBP with respect to the position and intensity of the various bands have been interpreted in terms of different molecular orbitals and energies involved in the excitations. In the MBP conformers, reduced coplanarity of the phenyl moiety with the carbonyl group increases the character of the $\pi_{Bz} \rightarrow \pi_{Bz}^*$ component of the relevant transition, resulting in a strong blue shift and a reduction of the oscillator strength. In HBP, on the other hand, the coplanarity of the two moieties lowers the energy of the π_{CO}^* orbital and results in a red shift for all transitions with respect to the MBP conformers. The hydrogen bond in HBP is mainly responsible for the coplanarity of the systems and strongly influences its spectroscopic behaviour. In MBP, on the other hand, the methyl group is an obstacle to coplanarity. For these reasons, the tail of the absorption band of HBP estimated at 3.53 eV is responsible for the yellow colour, whereas none of the MBP conformers show any absorption in the visible range of the spectrum.

Solvatochromism is predicted to red-shift all of the low-energy strong $\pi \rightarrow \pi_{CO}^*$ transitions in HBP and MBP because of the larger dipole moments of the excited states than the ground state. Differential effects for methanol compared with cyclohexane associated with the larger dielectric constant of the former are relatively small but are in qualitative agreement with the trends observed in the experimental spectra.

Acknowledgements

This work has been supported by the Italian Ministero dell'Istruzione dell'Università e della Ricerca (MIUR) and by the US National Science Foundation (NSF CHE02-03346).

The authors are grateful to Björn Roos for helpful discussion on the multiconfigurational perturbation theory and to the LUNARC center at Lund University (Sweden) for the usage on their cluster.

REFERENCES

1. Takeda R. *J. Am. Chem. Soc.* 1958; **80**: 4749–4750.
2. Petruso S, Bonanno S, Caronna S, Ciofalo M, Maggio B, Schillaci D. *Heterocycl. Chem.* 1994; **31**: 941–945.
3. Durham DG, Hughes CG, Rees AH. *Can. J. Chem.* 1972; **50**: 3223–3228.
4. Mahboobi S, Pongratz H, Hufsky H, Hockemeyer J, Frieser M, Lyssenko A, Paper D, Buergermeister J, Boehmer F-D, Fiebig H-H, Burger AM, Baasner S, Beckers T. *J. Med. Chem.* 2001; **44**: 4535–4553.
5. Beckers T, Reissmann T, Schmidt M, Burger A, Fiebig H, Vanhoefer U, Pongratz H, Hufsky H, Hockemeyer J, Frieser M, Mahboobi S. *Cancer Res.* 2002; **62**: 3113–3119.
6. Renneberg B, Kellner M, Laatsch H. *Ann. Chem.* 1993; 847–852.
7. Ciofalo M, La Manna G. *J. Mol. Struct. (Theochem.)* 2004; **709**: 183–186.
8. Roos BO. In *Advances in Chemical Physics: Ab Initio Methods in Quantum Chemistry*, vol. II, Lawley KP (ed.). Wiley: Chichester, 1987; 399–445.
9. Andersson K, Malmqvist P-Å, Roos BO, Sadlej AJ, Wolinski K. *J. Phys. Chem.* 1990; **94**: 5483–5488.
10. Andersson K, Malmqvist, P-Å, Roos BO. *J. Chem. Phys.* 1992; **96**: 1218–1226.
11. Roos BO, Andersson K, Fülscher MP, Malmqvist P-Å, Serrano-Andrés L, Pierloot K, Merchán M. In *Advances in Chemical Physics: New Methods in Computational Quantum Mechanics*, vol. XCIII, Prigogine I, Rice SA (eds). Wiley: New York, 1996; 219–331.
12. Pierloot K, Dumez B, Widmark P-O, Roos BO. *Theor. Chim. Acta.* 1995; **90**: 87–114.
13. Karlström G, Lindh R, Malmqvist P-Å, Roos BO, Ryde U, Veryazov V, Widmark P-O, Cossi M, Schimmelpfennig B, Neogrady P, Seijo L. *Comput. Mater. Sci.* 2003; **28**: 222–239.
14. Cramer CJ, Truhlar DG. *Chem. Rev.* 1999; **99**: 2161–2200.
15. Cramer CJ. In *Essentials of Computational Chemistry: Theories and Models* (2nd edn). Wiley: Chichester, 2004.
16. Li J, Williams B, Cramer CJ, Truhlar DG. *J. Chem. Phys.* 1999; **110**: 724–733.
17. Li J, Zhu T, Cramer CJ. *J. Phys. Chem. A* 1998; **102**: 1820–1831.
18. Li J, Zhu T, Cramer CJ. *J. Phys. Chem. A* 2000; **104**: 2178–2182.
19. Li J, Cramer CJ, Truhlar DG. *Int. J. Quantum Chem.* 2000; **77**: 264–280.
20. Zerner MC, Ridley JE, Bacon AD, Edwards WD, Head JD, McKelvey J, Culberson JC, Knappe P, Cory MG, Weiner B, Baker JD, Parkinson WA, Kannis D, Yu J, Roesch N, Kotzian M, Tamm T, Karelson MM, Zheng X, Pearl G, Broo A, Albert K, Cullen JM, Li J, Hawkins GD, Thompson JD, Liotard DA, Cramer CJ, Truhlar DG. *ZINDO-MN1.1*, *Quantum Theory Project*. University of Florida, Gainesville, and Department of Chemistry, University of Minnesota, Minneapolis, 2002.
21. Parr RG, Yang W. In *Density Functional Theory of Atoms and Molecules*. Oxford University Press: New York, 1989.
22. Becke AD. *Phys. Rev. A* 1988; **38**: 3098–3100.
23. Lee C, Yang W, Parr RG. *Phys. Rev. B* 1988; **37**: 785–789.
24. Hehre WJ, Radom L, Schleyer PvR, Pople JA. *Ab Initio Molecular Orbital Theory*. Wiley: New York, 1986.
25. Frisch MJ, Trucks GW, Schlegel HB, Scuseria GE, Robb MA, Cheeseman JR, Zakrzewski VG, Montgomery JA Jr, Stratmann RE, Burant JC, Dapprich S, Millam JM, Daniels AD, Kudin KN, Strain MC, Farkas O, Tomasi J, Barone V, Cossi M, Cammi R, Mennucci B, Pomelli C, Adamo C, Clifford S, Ochterski J, Petersson GA, Ayala PY, Cui Q, Morokuma K, Malick DK, Rabuck AD, Raghavachari K, Foresman JB, Cioslowski J, Ortiz JV, Baboul AG, Stefanov BB, Liu G, Liashenko A, Piskorz P, Komaromi I, Gomperts R, Martin RL, Fox DJ, Keith T, Al-Laham MA, Peng CY, Nanayakkara A, Challacombe M, Gill PMW, Johnson B, Chen W, Wong MW, Andres JL, Gonzalez C, Head-Gordon M, Replogle ES, Pople JA. *Gaussian 98*. Gaussian: Pittsburgh, PA, 1998.
26. Schaftenaar G, Noordik JH. *J. Comp.-Aided Mol. Design* 2000; **14**: 123–134.
27. Merchán M, Roos BO. *Theor. Chim. Acta* 1995; **92**: 227–239.
28. Merchán M, Roos BO, McDiarmid R, Xing X. *J. Chem. Phys.* 1996; **104**: 1791–1804.
29. Sobolewsky AL, Domcke W. *J. Phys. Chem. A* 1999; **103**: 4494–4504.
30. Molina V, Merchán M. *J. Phys. Chem. A* 2001; **105**: 3745–3751.
31. Nagaoka S, Hirota N, Sumitami M, Yoshihara K, Lipczynska-Kochany E, Iwamura H. *J. Am. Chem. Soc.* 1984; **106**: 6913–6916.
32. Sobolewsky AL, Domcke W. *Phys. Chem. Chem. Phys.* 1999; **1**: 3065–3072.
33. Hiraya A, Shobatake K. *J. Chem. Phys.* 1991; **94**: 7700–7706.
34. Chadwick DJ. In *The Chemistry of Heterocyclic Compounds: Pyrroles*, Jones RA (ed.). Wiley: Chichester, 1990: 38.

